Characterization of Zr-Al Substituted M-Type Barium Hexaferrite Synthesized by Co-Precipitation Method

Humaira Akhtar Shahia[1], Muhammad Shahzad Shifa[2*], Zeshan Mehboob[1], Muhammad Hashim[2], Faseeh ur Raheem[2]

[1] Department of Physics, Govt College University Faisalabad, Allama Iqbal Road, Faisalabad, Pakistan
[2] Institute of Physics, The Islamia University of Bahawalpur, Bahawalpur, Pakistan

ARTICLE INFO	ABSTRACT
	Structural properties of Zr-Al substituted M-type of barium hexaferrites, having compositions $Ba_{1-x}Zr_{0.5x}Al_{0.3}Fe_{11.7}O_{19}$, (x= 0.0, 0.1, 0.2, 0.3, 0.4, 0.5) are studied, which were synthesized by using co-precipitation method. These prepared samples are characterized by X-RAY diffraction (XRD) to confirm hexaferrites structure. Fourier transform infrared spectroscopy is used to make tetrahedral (higher frequency band) and octahedral (lower frequency band) clusters of metal oxides in hexaferrites and confirmed the formation of hexaferrites structure. (FESEM) Field emission scanning electron microscopy was used to give micrographs to show that grains are platelet like shaped, which agrees very well with hexaferrites structure. The particle morphology is observed to be porous and non-uniform. The grain size is decreased initially, and then increased with Zirconium additions. Scherer's formula is applied to calculate particle size, which is observed to change in the range of 18.86 nm-9.43 nm. The grains are bounded together due to interfacial surface tension forces. The optical properties are also studied by UV Vis spectrometer to find the energy band gap, in the range of 2.09ev - 5.15ev and absorbance peak having the range 237.9nm - 252.13nm. This change in energy band gap and absorbance peak is due to the change in the grain size on the zirconium substitution.

Corresponding Author's Email: shahzad.shifa@gmail.com

1. Introduction

Nano particles are being widely used in modern technology of our daily used appliances. Nano particles are actually atoms/molecules bonded together having radius less than 100 nm. Nano particles, called ferrites are ceramic compounds made up of oxides having iron as main component. Ferrites may be soft or hard magnetic materials. They are extremely magnetic in nature. Ferrites are classified into Spinel ferrites, Garnets, Ortho ferrites and hexaferrites. Among these ferrites, only hexagonal ferrites are hard ferrites and others are soft ferrites.

We used hard ferrites in our research. Hexagonal ferrites ($MeFe_{12}O_{19}$) can be further divided into M-type ($BaFe_{12}O_{19}$), Y-type ($Ba_2Me_2Fe_{12}O_{22}$), W-type ($BaMe_2Fe_{16}O_{27}$), X-type ($Ba_2Me_2Fe_{28}O_{46}$), Z-type ($Ba_3Me_2Fe_{24}O_{41}$) and U-type ($Ba_4Me_2Fe_{36}O_{60}$) by (Özgür, Alivov, & Morkoç, 2009; Smit & Wijn, 1959). M-Type Barium hexaferrites ($BaFe_{12}O_{19}$) are the most important series of the hard ferrites which has a wide range of applications, such as in permanent magnets (Litsardakis, Manolakis, Serletis, & Efthimiadis, 2008), loud speakers, ID cards etc.

These applications are due to their large coercivity (Livingston, 1981), high saturation and magnetization and easier synthesis etc. these M- Type barium hexaferrites are also used in magnetic recording applications due to their low manufacturing cost for industrial production and chemical stability (Ahmed, Okasha, & Kershi, 2008; Yamamoto, Nagakura, & Terada, 1990).

They are widely used in magnetic sensors electrodes, entertainment applications, photo-catalytic activity, hyperthermia applications, pollution control and drug delivery applications (Arruebo, Fernández-Pacheco, Ibarra, & Santamaría, 2007) etc. The improvement in structural and magnetic properties of these hard ferrites, e.g. corcivity, remanence, crystallite size etc. depend upon their method of synthesis and substitution of divalent or trivalent cations, particularly Ba^{+2}/Fe^{+3} ions. (Bsoul & Mahmood, 2009; Lee et al., 2010; Sözeri, 2009). The large anisotropy is also reduced by substitution of Fe^{+3} and/or Ba^{+2} by other metal cations to make them most stable for magneto optical recording media due to their microwave absorption properties. The M-Type hexaferrites consists of a unit cell with the lattice parameter a=5.88 Å and c= 23.2 Å. Our research belongs to M-Type barium hexaferrites ($BaFe_{12} O_{19}$) which depends upon the magnetic character (Fe^{+3} ion) having magnetic moment 5 µB. Each unit cell consists of 64 ions: 38 ions of oxygen, 24 ions Fe (iron) and one Me ion (Me= Ba^{2+}, Pb^{2+}, Sr^{2+} and La^{2+}). Ferric ions lie at 5 sites named as 2a, 2b, $4f_1$, $4f_2$ and 12k. Here 2a, $4f_2$ and 12k are octahedral, $4f_1$ is tetrahedral and 2b with 5 surrounding oxygen atoms form Trigonal bi pyramid. The oxygen atoms lie at 4e, 4f, 6h and 12k sites to form closed packed lattice. The Me ions occupy the 2d sites. Out of 12 Fe^{+3} ions in a formula unit, 6 Fe^{+3} lie at 12k sites and have spin up. 2, 2 ions lie at $4f_1$ and $4f_2$ sites with spin down while 1, 1 ion lies at 2a and 2b sites with spin up. So, out of 8 Fe^{+3} ions, having spin up (parallel to c-axis), 4 Fe^{+3} ions are cancelled out by Fe^{+3} ions with spin down. The remaining 4 Fe^{+3} ions, each with 5 unpaired electrons, give rise to 20µB magnetic moment per formula unit. The most commonly used and effectively methods to prepare these M-Type barium hexaferrites are high energy ball milling method (Ketov, Yagodkin, Lebed, Chernopyatova, & Khlopkov, 2006), sol-gel method (Abbas et al., 2015), Co-precipitation technique (Jotania & Patel, 2012), hydro thermal (Ataie, Harris, & Ponton, 1995), and chemical mixing (Dushaq et al., 2013) etc.

Among all these methods, co-precipitation technique is the simplest, most effective, cheap, direct and controllable method to prepare hexaferrites. Our present research is about to characterize Zr-Al substituted M-Type barium hexaferrites, having formula $Ba_{1-x}Zr_{0.5x} Al_{0.3} Fe_{11.7} O_{19}$, (x= 0.0, 0.1, 0.2, 0.3, 0.4, 0.5) synthesized by co-precipitation method. The objective of present work is to study the variation in structural, optical and magnetic properties of Zr-Al substituted M-type barium hexaferrite with the addition of zirconium in place of barium, which was not investigated before this, as according to the best of our knowledge.

2. Experimental Procedure

$Ba_{1-x}Zr_{0.5x} Al_{0.3} Fe_{11.7} O_{19}$ hexaferrites with (x= 0.0, 0.1, 0.2, 0.3, 0.4, 0.5) were prepared by using co-precipitation method. The chemicals used were $Ba(No_3)_2$ (Barium Nitrate), $ZrCl_4$ (Zirconium Chloride), $Fe(No_3)_3.9H_2o$(Iron Nitrate), $Al_2(No_3)$ (Aluminum Nitrate), NaOH (Sodium hydroxide). And DIW (Deionized water) (H_2O) was also used to make the precursors. All the metal nitrates and chlorides with particular stoichiometric ratio (according the formula) were mixed in 1000 ml beakers containing de ionized water. The solutions were made by shaking and heating all the ingredients at about 50℃-60℃ at first, and then stirred magnetically on magnetic hot plates, to form homogenous solutions. The sodium hydroxide (NaOH) solution was used to drop in the prepared solution, to get PH of about 10-12. After heating it further for 5-6 hours and then cooling, we got precipitates. We washed them with de-ionized water 5-6 times, to remove nitrates and chlorides contents. When the PH value reached to about 7, the solution was filtered with filter paper to separate the precipitates. These precipitates were dried in oven at 90℃ for 8 hours. The dried samples were ground and mixed by mortar and pestle, for about 30 minutes. Then the samples were annealed in furnace at 950℃ for about 6 hours. After cooling them, these samples were again ground and mixed to make the fine powder. Then these are ready to be used for various characterization techniques to study different properties.

3. Characterizations
3.1. XRD Analysis

The XRD patterns of all the sintered samples of $Ba_{1-x}Zr_{0.5x}Al_{0.3}Fe_{11.7}O_{19}$, (x= 0.0, 0.1, 0.2, 0.3, 0.4, 0.5) for the angles 30°- 56° are shown below in figure 1. All the peaks of XRD patterns were observed at angles of about 30°, 32°, 34°, 35°, 36°, 40°, 54° and 56°. These peaks were well indexed and were compared with JCPDs file No. 033-1340 with space group $P6_3/mmc$ (194). These peaks were indexed to the crystal planes of M-type hexaferrites i.e., (110), (112), (114), (200), (203), (205), (217) and (2011) respectively. (Almessiere, Slimani, El Sayed, Baykal, & Ercan, 2019; Gunanto, Jobiliong, & Adi, 2016; Li, Qiao, Li, Liu, & Peng, 2013). The remaining small peaks are due to the impurities present in the raw material. The four more prominent peaks in the XRD pattern were selected to find various parameters, like crystallite size(D), x-ray density $\rho(x-ray)$, inter planer spacing (d), lattice parameters(a) and (c) and cell volume (V) etc. by using the following formulas:

$$d = \frac{\lambda}{2 sin P} \qquad (1)$$

$$D = \frac{K\lambda}{\beta_{(hkl)} COS P} \qquad (2)$$

$$\frac{1}{d^2} = \frac{4}{3}\frac{h^2+hk+k^2}{a^2} + \frac{l^2}{c^2} \qquad (3)$$

$$\rho(x-ray) = \frac{ZM}{N_A V} \qquad (4)$$

$$V = 0.8666 a^2 C \qquad (5)$$

Where λ is the x-ray wavelength which is equal to 1.5414Å, K is the shape factor and its value is equal to 0.89 for hexagonal structure. P is the Bragg' diffraction angle. β_{hkl} is FWHM (full wave half maxima) of respective plain. N_A is Avogadro's number (6.02×10^{23} g/mole). M is molecular weight and Z is no. of molecules or formula units per unit cell of hexaferrites and is equal to 2. (M. A. Almessier et al., 1982). ρ is the x-ray density. The density (ρ) of the hexaferrites must be about 5.4 gm/cm^3 (Ghzaiel, Dhaoui, Pasko, & Mazaleyrat, 2016). M-type hexaferrites, the lattice parameter (a) and (c) must have the value of about 5.8 Å and 23.2 Å respectively. The ratio a/c for pure m-type Ba hexaferrites must be equal to 3.935 (Chawla, Meena, Kaur, Mudsainiyan, & Yusuf, 2015). The cell volume was found by using eq. (3.5) given above. Average cell volume of pure hexaferrites must be about 690 $Å^3$ (Ashraf, Zhang, Abbas, & Murtaza, 2018). The average crystallite size D must be in the range 15 nm-60 nm (Almessiere et al., 2019; Gunanto et al., 2016; Mahmood & Bsoul, 2017; Wang et al., 2016). In all the samples, the crystallite size is found in the range of 9.43 nm-18.86 nm, the average cell volume of all the samples is in the range of 539.77($Å^3$) to 502.51($Å^3$).

Table 1
Samples' crystallite size, interplanar spacing, cell volume, and density

Samples	Crystallite size (D) (nm)	Interplanar spacing (d) (Å)	Cell volume (V) (Å)	Density (ρ) g/cm³
$BaAl_{0.3}Fe_{11.7}O_{19}$ x=0.0	15.64	2.38	539.77	6.786
$Ba_{0.9}Zr_{0.05}Al_{0.3}Fe_{11.7}O_{19}$ x=0.1	9.49	3.36	496.32	7.319
$Ba_{0.8}Zr_{0.1}Al_{0.3}Fe_{11.7}O_{19}$ x=0.2	9.43	2.36	519.43	6.935
$Ba_{0.7}Zr_{0.15}Al_{0.3}Fe_{11.7}O_{19}$ x=0.3	17	2.38	537.24	6.648
$Ba_{0.6}Zr_{0.2}Al_{0.3}Fe_{11.7}O_{19}$ x=0.4	18.86	2.38	533.99	6.631
$Ba_{0.5}Zr_{0.25}Al_{0.3}Fe_{11.7}O_{19}$ x=0.5	18.80	2.38	502.51	6.986

Both of these results prove our samples to be M-type hexaferrites according to the literature mentioned above and also best for high density recording media (Christy, Rewatkar, & Sawadh, 2017). The crystallite size (D) and the average cell volume (V) must decrease with the addition of zirconium (Zr^{+4}) in each sample, because zirconium is a nonmagnetic ion having ionic radius of 80 pm, while that of barium is 268 pm. So if barium is replaced by zirconium having smaller radius, the radius, crystallite size and hence the cell volume in our samples($Ba_{1-x}Zr_{0.5x}Al_{0.3}Fe_{11.7}O_{19}$, (x= 0.0, 0.1, 0.2, 0.3, 0.4, 0.5) must decrease (Christy et al., 2017). but we see that in first three samples, the crystallite size(D) decrease and then starts to increase. Similarly the cell volume (V) decreases in first two

samples, but decreases onwards. The reason may be due to the fact explained below; zirconium (Zr^{+4}) usually likes to occupy mostly 2b (bipyramidal sites) sites and a little $4f_1$ (tetrahedral sites) sites (Jancarik et al., 2011). These sites are already occupied by iron (Fe^{+3}) ions. Also as for barium in tetrahedral sites, zirconium (Zr^{+4}) ions are distributed probably between tetrahedral and octahedral sites and have no particular preference due to its d^o configuration (Kanagesan, Jesurani, Velmurugan, Prabu, & Kalaivani, 2012).
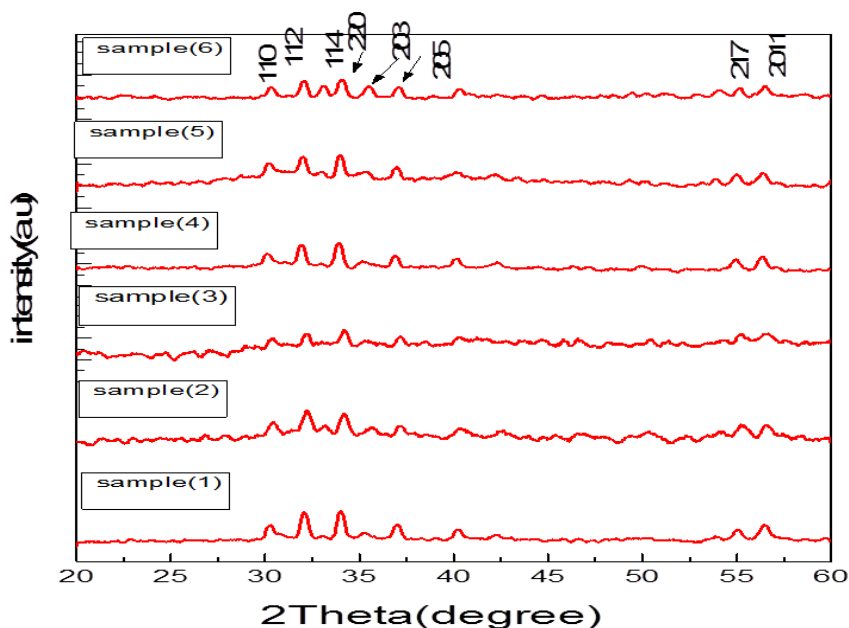
Figure 1: Xray diffraction peaks

Since the ionic radius of Fe^{3+} is 69 pm. Zirconium (having larger ionic radius as compared to iron (Fe^{3+})) substitutes Fe^{3+} at $4f_1$ site initially and then at 2b site afterwards, with the increasing Zr concentration. So, for both of these sites, substitution of zirconium, cause the particle size (D) and cell volume (V) to increase. Similarly the lattice parameter (a) and (c) of our samples are found in the range of 5.0 (Å) to 5.26 (Å) and 21.36 (Å) to 20.8(Å) respectively, which is in full agreement with the literature for M-type hexaferrites, stated above (Gunanto et al., 2016). We can see in table 2 that lattice parameters (a) and (c) decrease initially and then increase. Similarly, the density (ρ) has similar variations (increasing initially due to smaller particle size and cell volume but increasing laterally). Here also the reason may be due to the fact mentioned above, about the substitution of (Fe^{+3}) with (Zr^{+4}).

Table 2
The lattice parameters (a) and (c) with density (ρ) for $Ba_{1-x}Zr_{0.5x}Al_{0.3}Fe_{11.7}O_{19}$ (x=0.0, 0.1, 0.2, 0.3, 0.4, 0.5)

Samples	a (Å)	c (Å)	ρ (g/cm³)
x=0.0	5.40	21.36	6.786
x=0.1	5.26	20.70	7.319
x=0.2	5.34	21.02	6.935
x=0.3	5.40	21.26	6.648
x=0.4	5.39	21.21	6.631
x=0.5	5.28	20.8	6.986

3.2. FTIR Spectroscopy

FTIR (Fourier transformation infrared analysis) was performed to get structural phase information about the M-type hexaferrites. FTIR spectra for the samples $Ba_{1-x}Zr_{0.5x}Al_{0.3}Fe_{11.7}O_{19}$, (x=0.0, 0.1, 0.2, 0.3, 0.4, 0.5) are shown in figure 2, with the range $400cm^{-1}$-$4000cm^{-1}$ of wave number. The two main absorption bands v_1 and v_2, typical for hexagonal ferrites, were observed in the range $410.39cm^{-1}$-$451.59cm^{-1}$ and $572.76cm^{-1}$-$604.75cm^{-1}$ which may result due to intrinsic stretching vibrations of oxygen and metal ion (Fe-O), and are in octahedral and tetrahedral sites respectively (Chawla et al., 2015). The existence of these bands confirms the hexaferrites structure of our sample (Veisi, Yousefi, Amini, Shakeri, & Bagherzadeh, 2019). The bands range of $3200cm^{-1}$-$3500cm^{-1}$ shows the

presence of O-H group or moisture.in the samples (Almessiere et al., 2019; Li et al., 2013). Absence of this range in our samples shows that the reactions were completed. The slight bending at $948.61 cm^{-1}$, $1394.17 cm^{-1}$ and $1534.21 cm^{-1}$ show the weak bonds of C-O, $-CH_3$ and C-H respectively (Aparna, 2016; Temuujin et al., 2004), which may be present in the starting materials.
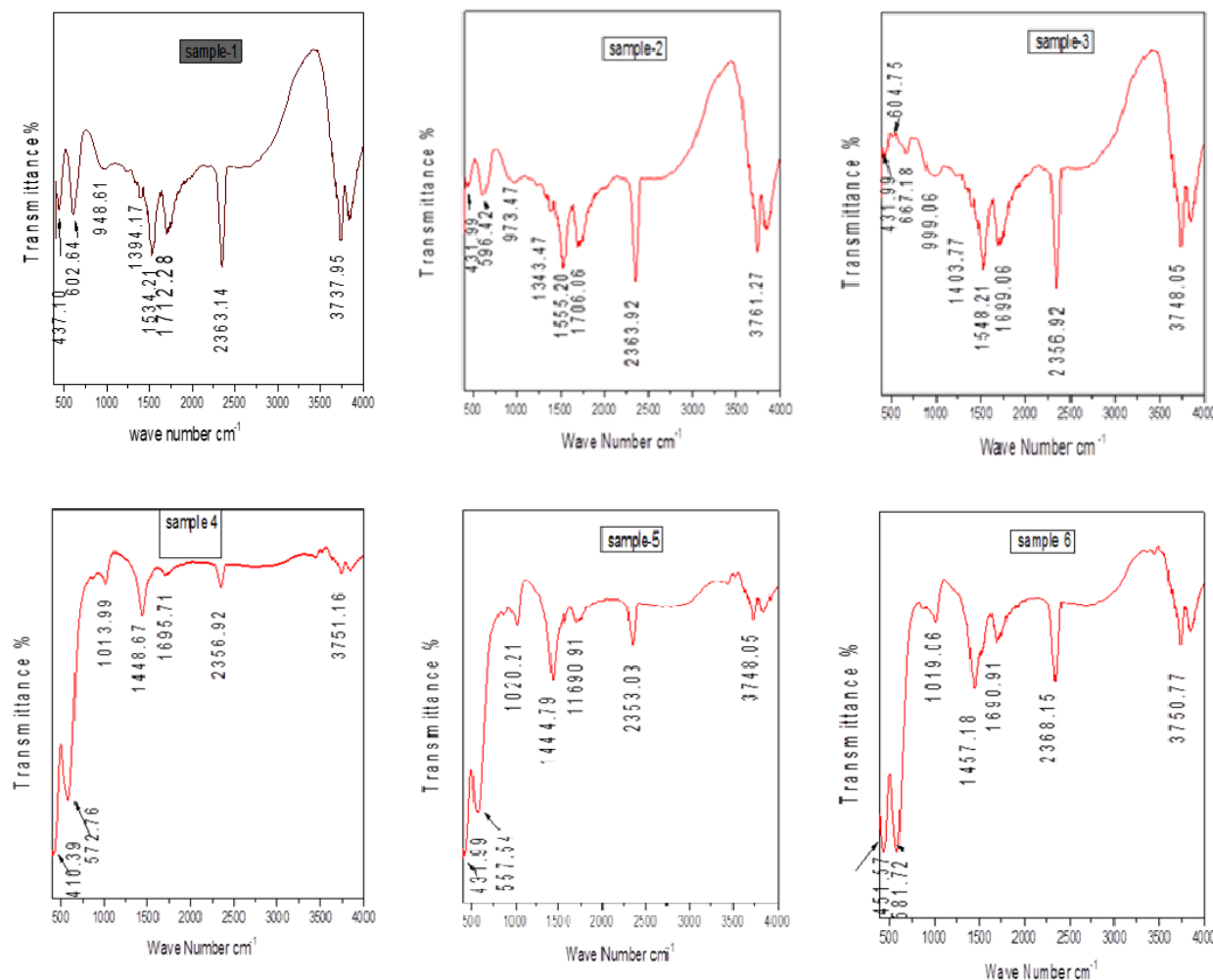
Figure 3.2: FTIR spectra for the samples $Ba_{1-x}Zr_{0.5x}Al_{0.3}Fe_{11.7}O_{19}$ (x=0.0, 0.1, 0.2, 0.3, 0.4, 0.5)

3.3. Scanning Electron Microscopy (SEM)

The SEM micrograph of all our samples $Ba_{1-x}Zr_{0.5x}Al_{0.3}Fe_{11.7}O_{19}$, (x=0.0, 0.1, 0.2, 0.3, 0.4, 0.5) are shown in figure 3 given below. As it is clear from the SEM micrographs, particles of all the samples are plate like, with hexagonal irregular shape and compact arrangement (Aparna, 2016). The plate like structure is the characteristics of hexaferrites (Topkaya, Auwal, & Baykal, 2016). The morphology of the particles and their grain size appears to be porous, non-uniform and show agglomerations, which agrees very well with the literature. This morphology may arise due to the fact that the particles of our hexaferrites samples are smaller in size and magnetic in nature (Temuujin et al., 2004). The overall view of the micrographs shows the particle size to decrease initially, which is the result of the addition of smaller size zirconium (Zr^{+4}) ions in place of barium having larger radii. (Christy et al., 2017). And then particle size seems to increase due to substitution of iron (Fe^{+3}) with zirconium (Zr^{+4}), as zirconium has no particular preference for occupation at tetrahedral site of barium or bi pyramid site of 2b or $4f_1$ of tetrahedral of iron (Fe^{+3}). In later cases particle size should increase due to larger ionic radius of Zr^{+4} as compared to (Fe^{+3}) (Gunanto et al., 2016).
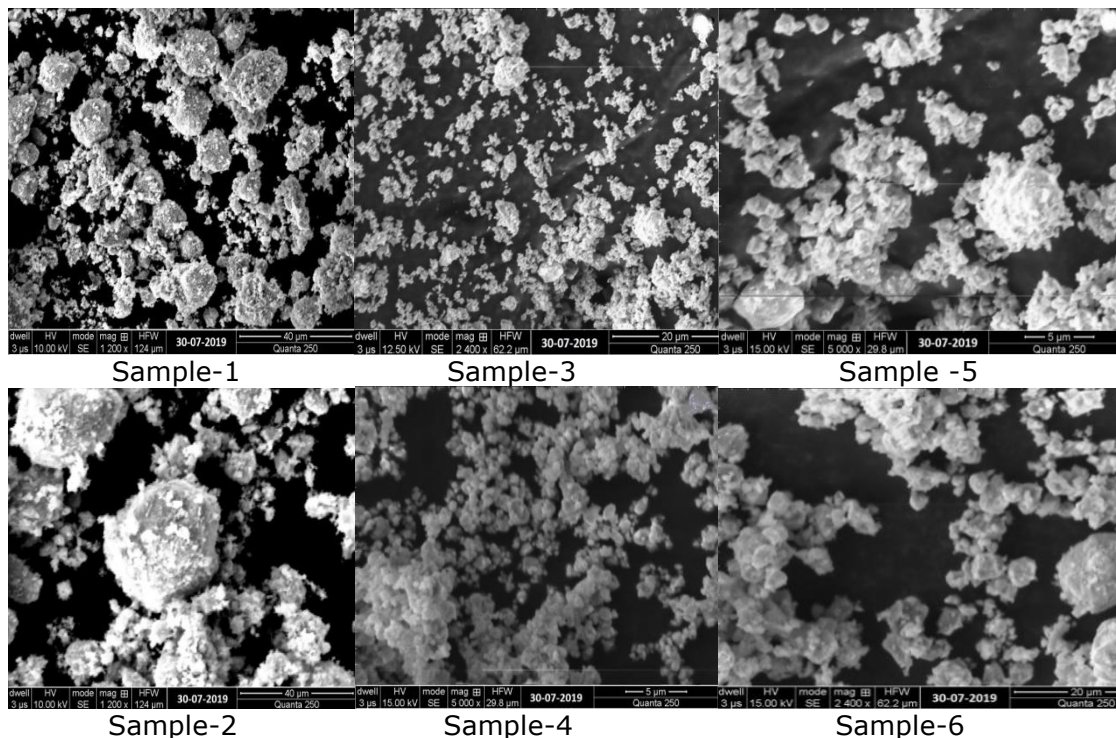
Figure 3: SEM micrograph of Ba$_{1-x}$Zr$_{0.5x}$Al$_{0.3}$Fe$_{11.7}$O$_{19}$, (x=0.0, 0.1, 0.2, 0.3, 0.4, 0.5)

3.4. UV Analysis

The prepared samples Ba$_{1-x}$Zr$_{0.5x}$Al$_{0.3}$Fe$_{11.7}$O$_{19}$, (x=0.0, 0.1, 0.2, 0.3, 0.4, 0.5) were analyzed by UV-Vis spectrometer. The optical band gap plots these samples are shown below in the figures 4. Optical properties of the samples were studied by using UV-Visible NIR technique in the range of 200 nm-1200 nm. The energy band gap was calculated by using Tauc method for each sample (Tauc, 1974). The energy band gap was in the range 2.09ev - 5.15ev, which is in full agreement with that of m-type hexaferrites (Ali et al., 2021). The energy band gap value for each sample is 2.09ev, 2.84ev, 5.15ev, 3.45ev, 3.30ev and 3.08ev respectively. This band gap variation may correspond to s, p, d spin exchange interactions among the delocalized s- or p- type band electrons of Fe and O atoms respectively and the localized d-electrons of the transition metal Zr ions, replacing the cations. Also, the initial increase in optical band gap energy depends upon the decrease in grain size of the nanoparticles at start, on the zirconium doping. (R. B. Bylsma., 1986). But afterwards the decrease in band gap energy may be due to increase in the crystallite size later on (Christy et al., 2017). Also, absorption peak lies between 237.9 nm -252.13 nm, which agrees very well with the above-mentioned literature.
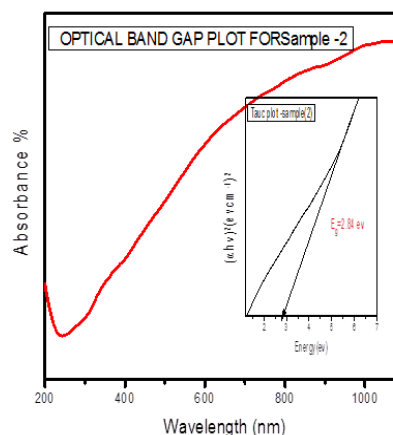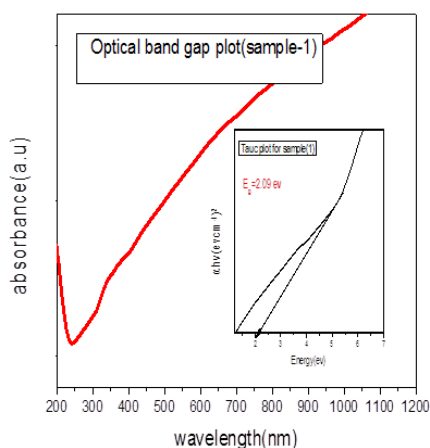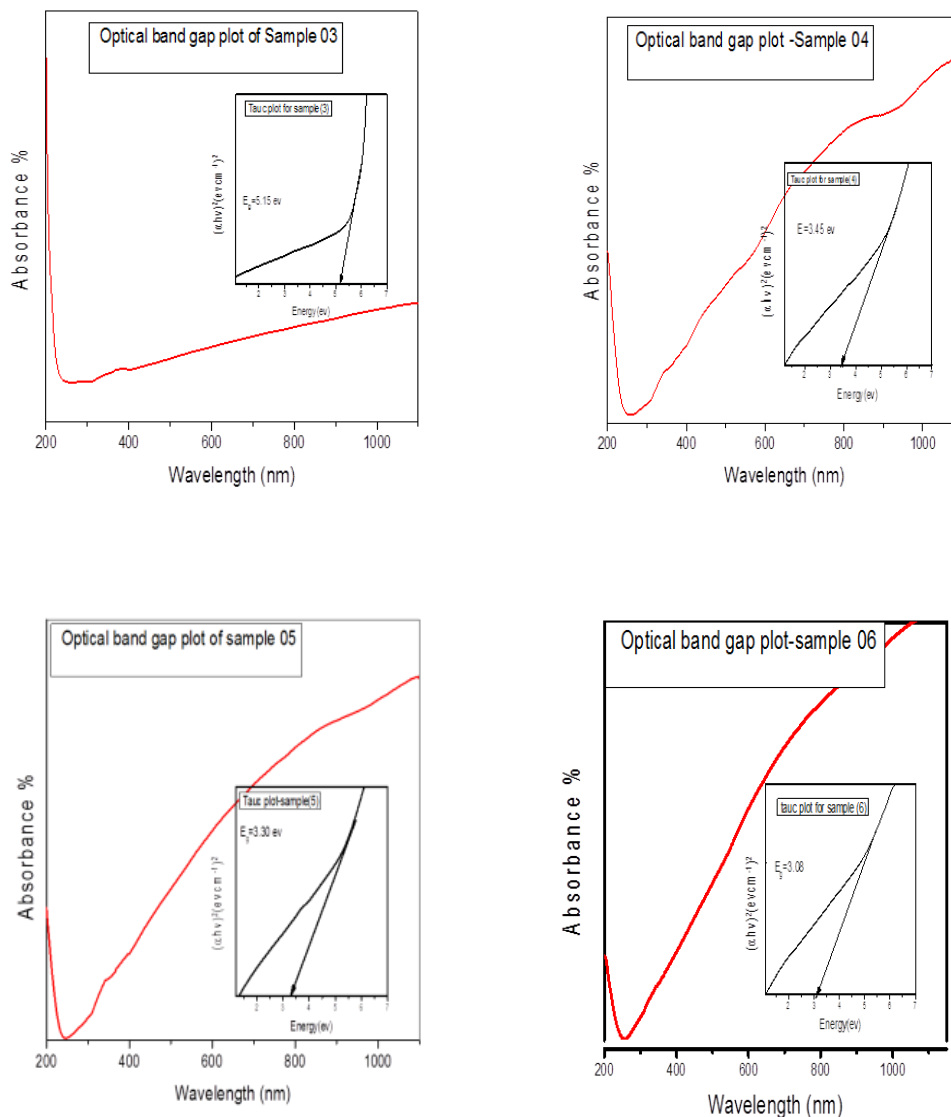
Figure 4: UV–Vis spectra of $Ba_{1-x}Zr_{0.5x}Al_{0.3}Fe_{11.7}O_{19}$ (x=0.0, 0.1, 0.2, 0.3, 0.4, 0.5)

4.   Conclusion

In our present work, Zr-Al substituted M-type barium hexaferrites $Ba_{1-x}Zr_{0.5x}Al_{0.3}Fe_{11.7}O_{19}$, (x=0.0, 0.1, 0.2, 0.3, 0.4, 0.5) are prepared by Co-precipitation method. We preferred this technique due to its low cost, effectiveness, particle size control quality. The XRD results confirmed their hexagonal structure. The lattice parameters a and c, cell volume and particle size were observed to decrease initially, due to zirconium addition and then starts to increase, which may be the result of substitution of zirconium (Zr^{+4}) with iron (Fe^{+3}), having smaller size. But the X-Ray density was observed to increase initially, with the zirconium addition but then decrease. It might be due to the above-mentioned reason. The crystallite size is found in the range of 9.43 nm-18.86 nm, which is the best for high density recording media. FTIR technique was used in the range of 400 cm^{-1}-4000 cm^{-1}. Two particular bands in the range 400 cm^{-1}-600 cm^{-1} confirmed the M-type hexagonal structure formation. The SEM images showed the particles were, mostly, plate like structured. Therefore, the hexaferrites formation was confirmed. SEM images also showed the decrease in grain size of the Nano particles initially, and then grain size is decreased, which agrees very well with the XRD results. UV Visible spectrum analysis provided the information about the optical properties of our Nanomaterial sample. The energy band gap was found in the range of 2.09 ev-5.15 ev and absorption peaks lie between the range 237 nm-252.13 nm. This variation in energy band gap and absorbance peaks, is due to the variations in particle size on zirconium addition and agrees well with the energy band gap variation in M-type barium hexaferrites.

References

Abbas, W., Ahmad, I., Kanwal, M., Murtaza, G., Ali, I., Khan, M. A., . . . Ahmad, M. (2015). Structural and magnetic behavior of Pr-substituted M-type hexagonal ferrites synthesized by sol–gel autocombustion for a variety of applications. *Journal of Magnetism and Magnetic Materials, 374*, 187-191. doi:10.1016/j.jmmm.2014.08.029

Ahmed, M., Okasha, N., & Kershi, R. (2008). Influence of rare-earth ions on the structure and magnetic properties of barium W-type hexaferrite. *Journal of Magnetism and Magnetic Materials, 320*(6), 1146-1150. doi:10.1016/j.jmmm.2007.11.014

Ali, H. T., Ramzan, M., Arshad, M. I., Morley, N. A., Abbas, M. H., Yusuf, M., . . . Amin, N. (2021). Tailoring the optical, and magnetic properties of La-BaM hexaferrites by Ni substitution. *Chinese Physics B*.

Almessiere, M., Slimani, Y., El Sayed, H., Baykal, A., & Ercan, I. (2019). Microstructural and magnetic investigation of vanadium-substituted Sr-nanohexaferrite. *Journal of Magnetism and Magnetic Materials, 471*, 124-132. doi:10.1016/j.jmmm.2018.09.054

Aparna, D. B., D. Kartikeyan, Dr. Moneesha Fernandes. (2016). Synthesis and Structural , Morphological & FTIR Studies on Ferrite Powders Bafe (12 − X) Ti X o 1 9 , Using Sol-Gel Method. *iosrjournals.org*.

Arruebo, M., Fernández-Pacheco, R., Ibarra, M. R., & Santamaría, J. (2007). Magnetic nanoparticles for drug delivery. *Nano today, 2*(3), 22-32. doi:10.1016/S1748-0132(07)70084-1

Ashraf, G. A., Zhang, L., Abbas, W., & Murtaza, G. (2018). Synthesis and characterizations of Al-Sm substituted Ba-Sr M-type hexagonal ferrite nanoparticles via sol-gel route. *Ceramics International, 44*(15), 18678-18685. doi:10.1016/j.ceramint.2018.07.096

Ataie, A., Harris, I., & Ponton, C. (1995). Magnetic properties of hydrothermally synthesized strontium hexaferrite as a function of synthesis conditions. *Journal of materials science, 30*(6), 1429-1433. doi:10.1007/BF00375243

Bsoul, I., & Mahmood, S. (2009). Structural and Magnetic Properties of BaFe12-x A1x O19 Prepared by Milling and Calcination.

Chawla, S., Meena, S., Kaur, P., Mudsainiyan, R., & Yusuf, S. (2015). Effect of site preferences on structural and magnetic switching properties of CO–Zr doped strontium hexaferrite SrCoxZrxFe (12− 2x) O19. *Journal of Magnetism and Magnetic Materials, 378*, 84-91. doi:10.1016/j.jmmm.2014.10.168

Christy, J., Rewatkar, K., & Sawadh, P. (2017). Influence of Zinc and Zirconium substitution on the structural and magnetic properties of Calcium hexaferrites.

Dushaq, G., Mahmood, S., Bsoul, I., Juwhari, H., Lahlouh, B., & AlDamen, M. (2013). Effects of molybdenum concentration and valence state on the structural and magnetic properties of BaFe 11.6 Mo x Zn 0.4− x O 19 hexaferrites. *Acta Metallurgica Sinica (English Letters), 26*(5), 509-516. doi:10.1007/s40195-013-0075-2

Ghzaiel, T. B., Dhaoui, W., Pasko, A., & Mazaleyrat, F. (2016). Effect of non-magnetic and magnetic trivalent ion substitutions on BaM-ferrite properties synthesized by hydrothermal method. *Journal of Alloys and Compounds, 671*, 245-253. doi:10.1016/j.jallcom.2016.02.071

Gunanto, Y., Jobiliong, E., & Adi, W. A. (2016). *Composition and phase analysis of nanocrystalline BaxSr1-xFe12O19 (x= 1.0; 0.6; and 0.4) by using general structure analysis system.* Paper presented at the AIP Conference Proceedings.

Jancarik, V., Gruskova, A., Slama, J., Dosoudil, R., Gonzalez, A., & Mendoza, G. (2011). Characteristics of magnetic properties of substituted hexagonal ferrites. *Advances in Electrical and Electronic Engineering, 5*(1), 344-346.

Jotania, R. B., & Patel, P. A. (2012). Microstructure and dielectric properties of Mn substituted Sr2Cu2Fe12O22 (Cu2Y) hexaferrite powder. *International Journal of Engineering Research and Applications (IJERA), 2*(4), 494-498.

Kanagesan, S., Jesurani, S., Velmurugan, R., Prabu, S., & Kalaivani, T. (2012). Structural and magnetic properties of conventional and microwave treated Ni–Zr doped barium strontium hexaferrite. *Materials Research Bulletin, 47*(2), 188-192. doi:10.1016/j.materresbull.2011.11.053

Ketov, S., Yagodkin, Y. D., Lebed, A., Chernopyatova, Y. V., & Khlopkov, K. (2006). Structure and magnetic properties of nanocrystalline SrFe12O19 alloy produced by

high-energy ball milling and annealing. *Journal of Magnetism and Magnetic Materials, 300*(1), e479-e481. doi:10.1016/j.jmmm.2005.10.199

Lee, J., Fuger, M., Fidler, J., Suess, D., Schrefl, T., & Shimizu, O. (2010). Modeling of the write and read back performances of hexagonal Ba-ferrite particulate media for high density tape recording. *Journal of Magnetism and Magnetic Materials, 322*(24), 3869-3875. doi:10.1016/j.jmmm.2010.08.010

Li, W., Qiao, X., Li, M., Liu, T., & Peng, H. (2013). La and Co substituted M-type barium ferrites processed by sol–gel combustion synthesis. *Materials Research Bulletin, 48*(11), 4449-4453. doi:10.1016/j.materresbull.2013.07.044

Litsardakis, G., Manolakis, I., Serletis, C., & Efthimiadis, K. (2008). High coercivity Gd-substituted Ba hexaferrites, prepared by chemical coprecipitation. *Journal of Applied Physics, 103*(7), 07E501. doi:10.1063/1.2832857

Livingston, J. (1981). A review of coercivity mechanisms. *Journal of Applied Physics, 52*(3), 2544-2548. doi:10.1063/1.328996

Mahmood, S., & Bsoul, I. (2017). Tuning the magnetic properties of M-type hexaferrites. *arXiv preprint arXiv:1707.07243*.

Özgür, Ü., Alivov, Y., & Morkoç, H. (2009). Microwave ferrites, part 1: fundamental properties. *Journal of Materials Science: Materials in Electronics, 20*(9), 789-834. doi:10.1007/s10854-009-9923-2

Smit, J., & Wijn, H. (1959). Ferrites, Philips Technical Library, Eindhoven. *The Netherlands, 151*, 157-158.

Sözeri, H. (2009). Simple recipe to synthesize single-domain BaFe12O19 with high saturation magnetization. *Journal of Magnetism and Magnetic Materials, 321*(18), 2717-2722. doi:10.1016/j.jmmm.2009.03.075

Tauc, J. (1974). Optical properties of amorphous semiconductors. In *Amorphous and liquid semiconductors* (pp. 159-220): Springer.

Temuujin, J., Aoyama, M., Senna, M., Masuko, T., Ando, C., & Kishi, H. (2004). Synthesis of Y-type hexaferrites via a soft mechanochemical route. *Journal of Solid State Chemistry, 177*(11), 3903-3908. doi:10.1016/j.jssc.2004.06.051

Topkaya, R., Auwal, I., & Baykal, A. (2016). Effect of temperature on magnetic properties of BaYxFe12− xO19 hexaferrites. *Ceramics International, 42*(14), 16296-16302. doi:10.1016/j.ceramint.2016.07.178

Veisi, S. S., Yousefi, M., Amini, M., Shakeri, A., & Bagherzadeh, M. (2019). Magnetic and microwave absorption properties of Cu/Zr doped M-type Ba/Sr hexaferrites prepared via sol-gel auto-combustion method. *Journal of Alloys and Compounds, 773*, 1187-1194. doi:10.1016/j.jallcom.2018.09.189

Wang, Y., Liu, Y., Li, J., Liu, Q., Zhang, H., & Harris, V. G. (2016). LTCC processed CoTi substituted M-type barium ferrite composite with BBSZ glass powder additives for microwave device applications. *AIP Advances, 6*(5), 056410. doi:10.1063/1.4945041

Yamamoto, H., Nagakura, M., & Terada, H. (1990). Magnetic properties of anisotropic Sr-La system ferrite magnets. *Ieee transactions on magnetics, 26*(3), 1144-1148. doi:10.1109/20.53989